Vibrational Spectroscopy of Mass-Selected [UO 2 (ligand) n] 2+ Complexes in the Gas Phase: Comparison with Theory

ARTICLE *in* JOURNAL OF THE AMERICAN CHEMICAL SOCIETY · MAY 2006

Impact Factor: 12.11 · DOI: 10.1021/ja058106n · Source: PubMed

9 AUTHORS, INCLUDING:

Kevin C. Cossel
University of Colorado Boulder
39 PUBLICATIONS **627** CITATIONS
SEE PROFILE

David T Moore
Lehigh University
53 PUBLICATIONS **1,619** CITATIONS
SEE PROFILE

Wibe A de Jong
Lawrence Berkeley National Laboratory
116 PUBLICATIONS **3,269** CITATIONS
SEE PROFILE

Lucas Visscher
VU University Amsterdam
151 PUBLICATIONS **4,099** CITATIONS
SEE PROFILE

J|A|C|S
ARTICLES
Published on Web 03/18/2006

Vibrational Spectroscopy of Mass-Selected $[UO_2(ligand)_n]^{2+}$ Complexes in the Gas Phase: Comparison with Theory

Gary S. Groenewold,*,† Anita K. Gianotto,† Kevin C. Cossel,†
Michael J. Van Stipdonk,‡ David T. Moore,§ Nick Polfer,§ Jos Oomens,§
Wibe A. de Jong,⊥ and Lucas Visscher#

Contribution from the Idaho National Laboratory, Idaho Falls, Idaho 83415-2208, Wichita State University, Wichita, Kansas, FOM Instituut voor Plasmafysica Rijnhuizen, Nieuwegein, The Netherlands, Pacific Northwest National Laboratory, Richland, Washington, and Vrije Universiteit Amsterdam, The Netherlands

Received December 9, 2005; E-mail: gary.groenewold@inl.gov

Abstract: The gas-phase infrared spectra of discrete uranyl ($[UO_2]^{2+}$) complexes ligated with acetone and/or acetonitrile were used to evaluate systematic trends of ligation on the position of the O═U═O stretch and to enable rigorous comparison with the results of computational studies. Ionic uranyl complexes isolated in a Fourier transform ion cyclotron resonance mass spectrometer were fragmented via infrared multiphoton dissociation using a free electron laser scanned over the mid-IR wavelengths. The asymmetric O═U═O stretching frequency was measured at 1017 cm^{-1} for $[UO_2(CH_3COCH_3)_2]^{2+}$ and was systematically red shifted to 1000 and 988 cm^{-1} by the addition of a third and fourth acetone ligand, respectively, which was consistent with increased donation of electron density to the uranium center in complexes with higher coordination number. The values generated computationally using LDA, B3LYP, and ZORA-PW91 were in good agreement with experimental measurements. In contrast to the uranyl frequency shifts, the carbonyl frequencies of the acetone ligands were progressively blue shifted as the number of ligands increased from two to four and approached that of free acetone. This observation was consistent with the formation of weaker noncovalent bonds between uranium and the carbonyl oxygen as the extent of ligation increases. Similar trends were observed for $[UO_2(CH_3CN)_n]^{2+}$ complexes, although the uranyl asymmetric stretching frequencies were greater than those measured for acetone complexes having equivalent coordination, which is consistent with the fact that acetonitrile is a weaker nucleophile than is acetone. This conclusion was confirmed by the uranyl stretching frequencies measured for mixed acetone/acetonitrile complexes, which showed that substitution of one acetone for one acetonitrile produced a modest red shift of 3−6 cm^{-1}.

Introduction

The chemical behavior of uranium is controlled by the structure and reactivity of an array of ligated complexes and clusters that is derived from competitive influences of 5f, 6d, and 7s orbitals on the metal center.[1−6] In solution, $[UO_2]^{2+}$ (uranyl, U(VI)) is the dominant species, but for this cation there is a multiplicity of interconverting species that complicates study in the condensed phases.[7,8] This has motivated extensive modeling efforts using computational chemistry at a variety of levels of theory and computing power.[9−13] However, it is frequently difficult to experimentally validate computational methods/approaches and calculated values, especially for actinide species.

Both Raman and infrared spectroscopy have been used to investigate ligand attachment to metal centers, starting with correlation of bond force constants with vibrational frequencies.[14] In the case of $[UO_2]^{2+}$, vibrational investigations are especially attractive because both the symmetric (ν_1) and asymmetric (ν_3) uranyl O═U═O stretching frequencies[15] serve

† Idaho National Laboratory.
‡ Wichita State University.
§ FOM Instituut voor Plasmafysica Rijnhuizen.
⊥ Pacific Northwest National Laboratory.
Vrije Universiteit Amsterdam.

(1) Brookins, D. G. *Geochemical Aspects of Radioactive Waste Disposal*; Springer-Verlag: New York, 1984.
(2) Burgess, J. *Metal Ions in Solution*; Ellis Horwood Limited: Chichester, U.K., 1978; p 481.
(3) Choppin, G. R.; Rizkalla, E. N. Solution Chemistry of Actinides and Lanthanides. In *Handbook on the Physics and Chemistry of Rare Earths*; Gschneider, J. K. A., Eyring, L., Choppin, G. R., Lander, G. H., Eds.; North-Holland: Amsterdam, 1994; Vol. 18, Lanthanides/Actinides: Chemistry, pp 559−590.
(4) Morse, J. W.; Choppin, G. R. *Rev. Aquat. Sci.* **1991**, *4* (1), 1−22.
(5) Schulz, W. W.; Navratil, J. D. *Science and Technology of Tributyl Phosphate*; CRC Press: Boca Raton, FL, 1984.
(6) Silva, R. J.; Nitsche, H. *Radiochim. Acta* **1995**, *70/71*, 377−396.
(7) Choppin, G. *Radiochim. Acta* **2004**, *92* (9−11), 519−523.
(8) Choppin, G. R.; Stout, B. E. *Sci. Total Environ.* **1989**, *83*, 203−216.
(9) Denning, R. G. *Struct. Bond.* **1992**, *79*, 215−276.
(10) Hay, P. J.; Martin, R. L.; Schreckenbach, G. *J. Phys. Chem. A* **2000**, *104*, 6259−6270.
(11) Kaltsoyannis, N. *Chem. Soc. Rev.* **2003**, *32* (1), 9−16.
(12) Pepper, M.; Bursten, B. E. *Chem. Rev.* **1991**, *91*, 719−741.
(13) Sonnenberg, J. L.; Hay, P. J.; Martin, R. L.; Bursten, B. E. *Inorg. Chem.* **2004**, *44*, 2255−2262.
(14) Badger, R. M. *J. Chem. Phys.* **1935**, *3*, 710−714.
(15) Jones, L. H. *Spectrochim. Acta* **1958**, *10*, 395−403.

10.1021/ja058106n CCC: $33.50

as sensitive "barometers" of the coordination environment of the actinide metal. The benchmark value of 965 wavenumbers (cm^{-1}) for the asymmetric stretch[16] was recorded for the aquo uranyl complex by Jones and Penneman using low pH, noncomplexing perchlorate solutions.[17] Subsequent measurements ranged from 954[18] to 962.5 cm^{-1},[19,20] probably on account of variations in the solution environment that supplies electron-donating ligands (solvent molecules and counteranions) that complex the uranyl and shift the stretching frequencies to lower values. McGlynn's measurements of O═U═O frequencies of uranyl salts led to the conclusion that donation of electron density into fδ and fϕ orbitals[12] resulted in repulsion of the axial oxygen atoms, with attendant decreases in the ν_1 and ν_3 frequencies.[21]

Changes in uranyl stretching frequencies have been correlated to the formation of ionic clusters in solution:[22] mono-, di- and triuranyl species were identified using the assumption of five equatorial ligands about the uranyl center in each case. A careful study of the Raman spectra of a variety of uranyl anion complexes by Nguyen-Trung et al. established a linear relationship between the red shift of the ν_1 (Raman) frequency and the number of ligands attached,[23] and this was later extended to the interpretation of the spectra of ionic clusters.[24] Toth and Begun had earlier shown that the ν_1 frequency decreased when ionic clusters containing multiple uranyl moieties were present.[25] Glebov examined both the ν_1 and the ν_3 frequencies, and derived relationships between the O═U═O force constants and equatorial bond distances.[26,27] These studies and those of Clark et al. established a correlation between uranyl stretch frequencies and the overall stability constants of these complexes, with the strongest nucleophiles producing the largest red shifts.[28] Clark et al. also showed that the red shift of the ν_1 frequency of the uranyl hydroxides in solution was larger than that observed in solid crystals,[28] demonstrating a significant influence on the stretching frequency by the solvent. This influence was substantiated further by the observation that axial oxygen atoms of the uranyl ion participate in exchange reactions with the solvent. The conclusions of these studies, with respect to influence of strongly donating ligands on stretching frequency, are in accord with red shifts to the uranyl ν_1 and ν_3 frequencies in hydroxyaromatic[29] and phosphine oxide coordination environments,[30] and at electron-donating surface sites on clays[31] and iron oxides,[32] to name a few additional examples.

In addition to complex formation, decreases of the O═U═O stretching frequencies are also generated by formal reduction of the U(VI) center (to U(V))[33,34] and by promotion of an electron into an excited state.[35] Shifts of 100 cm^{-1} or more have been attributed to both phenomena and support the conclusion that additional electrons in the valence shell of actinyl species red shift the frequencies.[36]

Computational studies have predicted significant red shifting of the IR-active ν_3 frequency as a result of ligand attachment to the uranyl center. Values calculated for bare $[UO_2]^{2+}$ asymmetric stretch varied from 1021 to as high as 1314 cm^{-1}, depending on the level of theory and the relativistic effective core potentials (ECPs) employed.[37] In a comparison of computational approaches, Marsden and co-workers calculated asymmetric stretch values for bare $[UO_2]^{2+}$ that ranged from 1060 to 1184 cm^{-1}.[38,39] Subsequent calculations of $[UO_2(ligand)_2]$ complexes using a very small relativistic effective core potential showed that as the ligand coordination energy increased, both the symmetric and asymmetric stretch frequencies decreased, consistent with donation of electron density from ligands to the uranyl center.[40] A red shift of 85 cm^{-1} was calculated for the asymmetric stretch of the diacetone complexes, which would put the unscaled value at ~1058 cm^{-1}; this value is noted because $[UO_2(acetone)_2]^{2+}$ is one of the species measured in the present study. Hay et al. compared several theoretical approaches for evaluating the pentaaquo complex $[UO_2(H_2O)_5]^{2+}$ and calculated asymmetric stretch values ranging from 1149 to 893 cm^{-1} (Hartree−Fock and B3LYP levels of theory, respectively),[10] and a similar range has been noted for $[UO_2(Cl)_4]^{2-}$.[41] Sonnenberg et al. employed a similar approach for tetra- and pentaligated uranyl complexes.[13] Starting with a value for the bare $[UO_2]^{2+}$ asymmetric stretch of 1129 cm^{-1}, they predicted that the tetrahydroxy complex $[UO_2(OH)_4]^{2-}$ would be red shifted to 829 cm^{-1}, sharply lower than the frequency of the tetraligated complex containing the much weaker CO donor, $[UO_2(CO)_4]^{2+}$, which was shifted only to 1069 cm^{-1}. Recently, de Jong et al. used local density functional theory to calculate structures and vibrational frequencies of carbonate, nitrate, and acetate complexes.[42] Starting from a frequency of 1123 cm^{-1} for the bare $[UO_2]^{2+}$, they calculated a systematic red shift upon serial addition of three ligands, producing values of 827, 934, and 948 cm^{-1} for the tricarbonate, triacetate, and trinitrate complexes (respectively). On the basis of consideration of both the computational results and the spectroscopic measurements, it is clear that the uranyl stretching frequencies are extremely valuable for diagnosing the coordination environment of the metal center. Yet it is difficult to draw

(16) Jones, L. H.; Penneman, R. A. *J. Chem. Phys.* **1953**, *21* (3), 542−544.
(17) Brooker, M. H.; Huang, C.-H.; Sylwestrowicz, J. *J. Inorg. Nucl. Chem.* **1980**, *42*, 1431−1440.
(18) Best, S. P.; Clark, R. J. H.; Cooney, R. P. *Inorg. Chim. Acta* **1988**, *145*, 141−147.
(19) Quiles, F.; Burneau, A. *Vib. Spectrosc.* **1998**, *18*, 61−75.
(20) Gal, M.; Goggin, P. L.; Mink, J. *J. Mol. Struct.* **1984**, *114*, 459−462.
(21) McGlynn, S. P.; Smith, J. K.; Neely, W. C. *J. Chem. Phys.* **1961**, *35* (1), 105−116.
(22) Quiles, F.; Burneau, A. *Vib. Spectrosc.* **2000**, *23*, 231−241.
(23) Nguyen-Trung, C.; Begun, G. M.; Palmer, D. A. *Inorg. Chem.* **1992**, *31* (25), 5280−5287.
(24) Nguyen-Trung, C.; Palmer, D. A.; Begun, G. M.; Peiffert, C.; Mesmer, R. E. *J. Solution Chem.* **2000**, *29* (2), 101−129.
(25) Toth, L. M.; Begun, G. M. *J. Phys. Chem.* **1981**, *85*, 547−549.
(26) Glebov, V. A. *Koord. Khim.* **1982**, *8* (7), 970−976.
(27) Glebov, V. A. *Koord. Khim.* **1981**, *7* (3), 388−395.
(28) Clark, D. L.; Conradson, S. D.; Donohoe, R. J.; Keogh, D. W.; Morris, D. E.; Palmer, P. D.; Rogers, R. D.; Tait, C. D. *Inorg. Chem.* **1999**, *38* (7), 1456−1466.
(29) Tellez Soto, C. A.; Arissawa, M.; Gomez, L. J.; Mondragon, M. A. *Polyhedron* **2000**, *19*, 2353−2360.
(30) Burns, C. J.; Smith, C. C.; Sattelberger, A. P.; Gray, H. B. *Inorg. Chem.* **1992**, *31*, 3724−3727.
(31) Morris, D. E.; Chisholm-Brause, C. J.; Barr, M. E.; Conradson, S. D.; Gary Eller, P. *Geochim. Cosmochim. Acta* **1994**, *58* (17), 3613−3623.
(32) Duff, M. C.; Coughlin, J. U.; Hunter, D. B. *Geochim. Cosmochim. Acta* **2002**, *66*, 3533−3547.
(33) Mizuoka, K.; Ikeda, Y. *Radiochim. Acta* **2004**, *92*, 631−635.
(34) Mizuoka, K.; Ikeda, Y. *Inorg. Chem.* **2003**, *42*, 3396−3398.
(35) Kasha, M. *J. Chem. Phys.* **1949**, *17* (3), 349.
(36) Basile, L. J.; Sullivan, J. C.; Ferraro, J. R.; LaBonville, P. *Appl. Spectrosc.* **1974**, *28* (2), 142−145.
(37) de Jong, W. A.; Harrison, R. J.; Nichols, J. A.; Dixon, D. A. *Theor. Chem. Acc.* **2001**, *107*, 22−26.
(38) Clavaguera-Sarrio, C.; Ismail, N.; Marsden, C. J.; Begue, D.; Pouchan, C. *Chem. Phys.* **2004**, *302*, 1−11.
(39) Ismail, N.; Heully, J.-L.; Saue, T.; Daudey, J.-P.; Marsden, C. J. *Chem. Phys. Lett.* **1999**, *300*, 296−302.
(40) Clavaguera-Sarrio, C.; Hoyau, S.; Ismail, N.; Marsden, C. J. *J. Phys. Chem. A* **2003**, *107*, 4515−4525.
(41) Schreckenbach, G.; Hay, P. J.; Martin, R. L. *J. Comput. Chem.* **1999**, *20*, 70−90.
(42) de Jong, W. A.; Apra, E.; Windus, T. L.; Nichols, J. A.; Harrison, R. J.; Gutowski, K. E.; Dixon, D. A. *J. Phys. Chem. A* **2005**, *109* (50), 11568−11577.

specific conclusions based on solution-phase measurements because of uncertainty arising from the possibility of multiple and potentially competing interactions occurring between the solvent and the dication.[43,44] Inner-sphere solvent exchange rates have been measured at 10^6 s^{-1},[43] and the coordination energy of complexes has contributions arising from factors derived from electrostatic attraction, repulsion, ligand polarization, uranyl polarization, charge transfer from the ligand to the uranyl, and reverse charge transfer.[40,44] However, an environment offering a greater degree of control, such as the gas phase, might enable measurement of vibrational frequencies that can be assigned to explicitly defined species, because the chemical complexity in the gas phase is considerably lower.

Mass spectrometry offers a partial solution to these difficulties: discrete solvent complexes can be generated and isolated in the gas phase so that the oxidation state and the number of ligands are defined. Beauchamp and co-workers conducted initial studies of low-valent U cations using an ion-beam instrument,[45−47] and this work was later expanded upon by Schwarz and co-workers who used Fourier transform mass spectrometry.[48,49] About the same time, Gibson and co-workers[50−61] began research using a similar approach to conduct extensive studies of the gas-phase reactions of actinide cations leading to bounding of bond energies. More recently, gas-phase reactivity studies conducted by Van Stipdonk and co-workers,[62−68] Moulin and co-workers,[69,70] and Pasilis and Pemberton[71] have provided insight into ligand preferences and extent of coordination in $[UO_2]^{2+}$ complexes, which were deduced from ligand substitution reactions and collision-induced dissociation (CID). These studies represent remarkable progress in gas-phase actinide chemistry but have not provided a more quantitative validation of the computational studies.

A conceptually attractive approach would be to compare experimental frequencies measured for discrete uranyl−ligand complexes in the gas phase with ab initio calculated values. Generally, the low photon flux of incident irradiation, together with low gas-phase concentrations, renders vibrational spectroscopy impractical for interrogation of charged species trapped in a mass spectrometer. However, the combination of high-intensity lasers combined with trapped ion mass spectrometers overcomes this limitation. The free electron laser for infrared experiments (FELIX) located at the FOM Instituut voor Plasmafysica "Rijnhuizen" (Nieuwegein, The Netherlands)[72] is interfaced to a Fourier transform ion cyclotron resonance (FT-ICR) mass spectrometer.[73] This instrumental combination enables acquisition of infrared multiphoton dissociation (IRMPD) spectra of gas-phase ions produced using either electrospray ionization or laser desorption and has proven to be an excellent technique for examining organics, metal complexes, and clusters.[73−77] Reported here are the first IR spectra of discrete gas-phase uranyl−solvent complexes, which quantitatively measure the effect of the number and type of electron-donating solvent ligands on the asymmetric O═U═O stretching frequency. The experimentally generated values for the asymmetric stretch serve as benchmarks for the validation and comparison of values calculated using several approaches and with IR values measured in solution.

Experimental Section

Generation of Uranyl Complexes by Electrospray Ionization (ESI). ESI was used to generate singly and doubly charged uranyl complexes.[63,68] A 1 mM solution of uranyl nitrate was generated by dissolving the hexahydrate salt (Fluka/Sigma-Aldrich, St. Louis, MO) in a 9:1 solution of water/organic as solvent, where the organic used was either acetone or acetonitrile. The ESI of these solutions produced $[UO_2(solvent)_n]^{2+}$ complexes containing all acetone or all acetonitrile. Mixed acetone−acetonitrile uranyl complexes were formed using the water/acetonitrile solution and leaking a trace amount of acetone into the ion accumulation region (hexapole). The ESI source (Micromass, Manchester, U.K.) was operated at 3 kV with respect to ground. Ions were generated at atmospheric pressure and were extracted into the vacuum and ion optics orthogonally with respect to the spray axis.

The ESI mass spectra of the uranyl complexes were sensitive to the desolvation temperature,[68] which was controlled by a heater and thermocouple on the block through which the spray capillary passed. At the lowest temperatures (i.e., at room temperature with the heater turned off), abundant, highly coordinated $[UO_2(ligand)_5]^{2+}$ complexes could be formed and transmitted through the ion accumulation chamber and into the FT-ICR-MS, which enabled acquisition of the O═U═O stretch of the $[UO_2(acetonitrile)_5]^{2+}$ complex. However, we were unable

(43) Farkas, I.; Banyai, I.; Szabo, Z.; Wahlgren, U.; Brenthe, I. *Inorg. Chem.* **2000**, *39*, 799−805.
(44) Hagberg, D.; Karlstrom, G.; Roos, B. O.; Gagliardi, L. *J. Am. Chem. Soc.* **2005**, *127*, 14250−14256.
(45) Armentrout, P.; Hodges, R.; Beauchamp, J. L. *J. Am. Chem. Soc.* **1977**, *99* (9), 3162−3163.
(46) Armentrout, P. B.; Beauchamp, J. L. *Chem. Phys.* **1980**, *50* (1), 27−36.
(47) Armentrout, P. B.; Hodges, R. V.; Beauchamp, J. L. *J. Chem. Phys.* **1977**, *66* (10), 4683−4688.
(48) Cornehl, H. H.; Heinemann, C.; Marcalo, J.; deMatos, A. P.; Schwarz, H. *Angew. Chem., Int. Ed. Engl.* **1996**, *35* (8), 891−894.
(49) Heinemann, C.; Cornehl, H. H.; Schwarz, H. *J. Organomet. Chem.* **1995**, *501* (1−2), 201−209.
(50) Gibson, J. K. *Int. J. Mass Spectrom. Ion Processes* **2002**, *213* (1), 1−21.
(51) Gibson, J. K. *J. Mass Spectrom.* **2001**, *36* (3), 284−293.
(52) Gibson, J. K. *Organometallics* **1997**, *16* (19), 4214−4222.
(53) Gibson, J. K. *J. Am. Chem. Soc.* **1998**, *120* (11), 2633−2640.
(54) Gibson, J. K. *J. Alloys Compd.* **1998**, *271*, 359−362.
(55) Gibson, J. K. *J. Vac. Sci. Technol., A* **1997**, *15* (4), 2107−2118.
(56) Gibson, J. K. *Radiochim. Acta* **1998**, *81* (2), 83−91.
(57) Gibson, J. K. *J. Mass Spectrom.* **1999**, *34* (11), 1166−1177.
(58) Jackson, G. P.; Gibson, J. K.; Duckworth, D. C. *Int. J. Mass Spectrom.* **2002**, *220*, 419−441.
(59) Jackson, G. P.; Gibson, J. K.; Duckworth, D. C. *J. Phys. Chem. A* **2004**, *108*, 1042−1051.
(60) McGinnis, C. P.; Hunt, R. D.; Gibson, S. M.; Gilchrist, R. L. *Sep. Sci. Technol.* **1995**, *30* (7−9), 1741−1754.
(61) Gibson, J. K.; Haire, R. G.; Santos, M.; Marcüalo, J.; Pires de Matos, A. *J. Phys. Chem. A* **2005**, *109*, 2768−2781.
(62) Anbalagan, V.; Chien, W.; Gresham, G. L.; Groenewold, G. S.; Van Stipdonk, M. J. *Rapid Commun. Mass Spectrom.* **2004**, *18*, 3028−3034.
(63) Chien, W.; Anbalagan, V.; Zandler, M.; Hanna, D.; Van Stipdonk, M.; Gresham, G.; Groenewold, G. *J. Am. Soc. Mass Spectrom.* **2004**, *15*, 777−783.
(64) Gresham, G. L.; Gianotto, A. K.; Harrington, P. d. B.; Cao, L.; Scott, J. R.; Olson, J. E.; Appelhans, A. D.; Van Stipdonk, M. J.; Groenewold, G. S. *J. Phys. Chem. A* **2003**, *107*, 8530−8538.
(65) Groenewold, G. S.; Van Stipdonk, M. J.; Gresham, G. L.; Hanna, D.; Chien, W.; Anbalagan, V. *J. Mass Spectrom.* **2004**, *39*, 752−761.
(66) Van Stipdonk, M.; Anbalagan, V.; Chien, W.; Gresham, G.; Groenewold, G.; Hanna, D. *J. Am. Soc. Mass Spectrom.* **2003**, *14* (11), 1205−1214.
(67) Van Stipdonk, M. J.; Chien, W.; Anbalagan, V.; Gresham, G. L.; Groenewold, G. S. *Int. J. Mass Spectrom.* **2004**, *237*, 175−183.
(68) Van Stipdonk, M. J.; Chien, W.; Angalaban, V.; Bulleigh, K.; Hanna, D.; Groenewold, G. S. *J. Phys. Chem. A* **2004**, *108*, 10448−10457.
(69) Jacopin, C.; Sawicki, M.; Plancque, G.; Doizi, D.; Taran, F.; Ansoborlo, E.; Amekraz, B.; Moulin, C. *Inorg. Chem.* **2003**, *42*, 5015−5022.
(70) Moulin, C.; Amekraza, B.; Hubert, S.; Moulin, V. *Anal. Chim. Acta* **2001**, *441*, 269−279.
(71) Pasilis, S. P.; Pemberton, J. E. *Inorg. Chem.* **2003**, *42*, 6793−6800.
(72) Oepts, D.; van der Meer, A. F. G.; van Amersfoort, P. W. *Infrared Phys. Technol.* **1995**, *36* (1), 297−308.
(73) Moore, D. T.; Oomens, J.; van der Meer, L.; von Helden, G.; Meijer, G.; Valle, J.; Marshall, A. G.; Eyler, J. R. *ChemPhysChem* **2004**, *5*, 740−743.
(74) Moore, D. T.; Oomens, J.; Eyler, J. R.; Meijer, G.; von Helden, G.; Ridge, D. P. *J. Am. Chem. Soc.* **2004**, *126*, 14726−14727.
(75) Oomens, J.; Moore, D. T.; von Helden, G.; Meijer, G.; Dunbar, R. C. *J. Am. Chem. Soc.* **2004**, *126*, 724−725.
(76) Oomens, J.; Tielens, A. G. G. M.; Sartakaov, B. G.; Von Helden, G.; Meijer, G. *Astrophys. J.* **2003**, *591*, 968−985.
(77) van Heijnsbergen, D.; Demyk, K.; Duncan, M. A.; Meijer, G.; von Helden, G. *Phys. Chem. Chem. Phys.* **2003**, *5*, 2515−2519.

to form the pentaacetone complex for the 1−3 h required for acquisition of IRMPD data. Acetone and acetonitrile complexes containing three and four ligands were stabilized more easily using a desolvation temperature of 80 °C and a desolvation flow (N_2) of 21 L min^{-1}. At higher desolvation temperatures, doubly charged uranyl complexes underwent charge reduction reactions.

Fourier Transform Ion Cyclotron Resonance Mass Spectrometry (FT-ICR-MS).[73−75] Ions were accumulated in an external hexapole for about 500 ms prior to being injected into the ICR cell. An envelope of singly and doubly charged uranyl complexes was formed that contained three, four, or five solvent ligands. Specified complexes were isolated using a stored waveform inverse Fourier transform (SWIFT) pulse,[78] which ejected all species except those having the desired mass. Complexes containing two acetone ligands were formed using sustained off-resonance irradiation (SORI) following a He gas pulse,[79] (typically pulsed between 3×10^{-7} and 1×10^{-6} Torr) which stimulated elimination of a solvent molecule from the complex by collision-induced dissociation. There was a concern that the IRMPD spectra may be influenced by vibrationally excited complexes formed by SORI. To evaluate this, spectra were acquired both before and after an ion cool-down step of about 1 s that was added between the SORI stage and irradiation by FELIX, which should allow the molecules to undergo substantial radiative cooling. No difference in the observed frequency was noted in the spectra, which supported the supposition that residual internal energy from the SORI-induced ligand elimination had dissipated or was not influencing photon absorption frequency. An additional observation that supports this conclusion is that the bandwidths observed are among the narrowest found in all our experiments in the FT-ICR as well as in a quadrupole ion trap (which operates at a much higher pressure). If the ions were internally hot, broader bands would have been expected.

Infrared Multiphoton Dissociation. Isolated ionic complexes were irradiated using two FELIX macropulses, which induced elimination of a solvent molecule from the complex when the incident wavelength matched an absorption band. The IRMPD mechanism has been described in detail elsewhere.[80] Briefly, it involves sequential, non-coherent absorption of many (from tens to hundreds) infrared photons, with each photon being "relaxed" by intramolecular vibrational redistribution before the next one is absorbed. In this way, the internal vibrational energy of the molecule can be resonantly pumped significantly above the dissociation threshold, resulting in fragmentation. It has been shown that the infrared spectra obtained are comparable to those obtained using linear absorption techniques.[75,76] FELIX was scanned between 5.2 and 12 μm in increments of ≤ 0.4 μm, after which IRMPD product ions and undissociated precursor ions were measured using the excite/detect sequence of the FT-ICR-MS.[81] The IRMPD efficiency was then expressed as $-\log(1 -$ (summed fragment ion yield)), corrected for the width of the acquisition channels and linearly normalized to correct for variations in FELIX power over the spectral range.

Density Functional Theory (DFT) Structure and Frequency Calculations Using B3LYP. The DFT geometry optimizations and frequency calculations using the Gaussian suite of programs[82] were performed at the B3LYP level of theory using the 6-31+G(d) basis for the O, C, H, and N atoms and the SDD basis set for U. The SDD basis set employs the Stuttgart/Dresden effective core potential[83−86] and has been effectively used by our group[63] for modeling uranium complexes. Comparative calculations showed that lowest energy conformations matched those reported in previous studies of similar systems using other basis sets.[87,88] The resulting frequencies were scaled by 0.975, which falls within the customary range of 0.95−0.98 generally suggested for calculations of this type,[89−92] to give optimal agreement with the IRMPD spectra. The basis set superposition error (BSSE) values for the mixed SDD/6-31+G(d) basis were calculated by the counterpoise method and found to be <1 kcal mol^{-1} per ligand. The geometries and frequencies of the smaller clusters ($n = 1$, 2) were checked using a much larger "maximal" mixed SDD/6-311++G(3df,-3pd); no significant discrepancies were found relative to the results using the smaller mixed basis.

DFT Structure and Frequency Calculations Using Local Density Approximation (LDA). DFT calculations using the NWChem[93,94] suite of programs were performed at the LDA[95,96] level of theory using the small core Stuttgart RECP and associated Stuttgart orbital basis set for U[83,86,97−102] and the valence triple-ζ plus polarization (TZVP) DFT optimized basis sets for all other atoms (O, C, H, and N).[103] In all cases, spherical basis sets were employed. No scaling of the calculated frequencies was performed.

Structure and Frequency Calculations Using ZORA-PW91. Vibrational frequencies at the ZORA-PW91 level of theory were calculated for the acetonitrile complexes.[104] In these calculations, we analyzed the uranyl−ligand bond according to the Ziegler−Rauk[105,106] energy decomposition[107] as is implemented in ADF2005.01.[108] No scaling of the calculated frequencies was performed.

Results and Discussion

IRMPD of Uranyl−Acetone (ACO) Complexes. The ESI-MS of uranyl nitrate in water/acetone produced dications having compositions $[UO_2(ACO)_n]^{2+}$ where $n = 3$ or 4 (Figure 1).

(78) Marshall, A. G.; Wang, T.-C. L.; Ricca, T. L. *J. Am. Chem. Soc.* **1985**, *107*, 7893−7897.
(79) Gauthier, J. W.; Trautman, T. R.; Jacobson, D. B. *Anal. Chim. Acta* **1991**, *246*, 211−225.
(80) Bagratashvili, V. N.; Letokov, V. S.; Makarov, A. A.; Ryabov, E. A. *Multiple Photon Infrared Laser Photophysics and Photochemistry*; Harwood: Chur, Switzerland,1985.
(81) Marshall, A. G.; Hendrickson, C. L.; Jackson, G. S. *Mass Spectrom. Rev.* **1998**, *17* (1), 1−35.
(82) Frisch, M. J.; et al. *Gaussion 98*, revision A.4; Gaussian, Inc.: Pittsburgh, PA, 1998.
(83) Bergner, A.; Dolg, M.; Küchle, W.; Stoll, H.; Preuss, H. *Mol. Phys.* **1993**, *80* (6), 1431−1441.
(84) Dolg, M. In *Modern Methods and Algorithms of Quantum Chemistry*; John von Neumann Institute for Computing: Jülich, Germany, 2000; Vol. 1, p 479.
(85) Dunning, T. H., Jr.; Hay, P. J. In *Modern Theoretical Chemistry*; Plenum: New York, 1976; Vol. 3.
(86) Küchle, W.; Dolg, M.; Stoll, H.; Preuss, H. *Mol. Phys.* **1991**, *74* (6), 1245−1263.
(87) Oda, Y.; Aoshima, A. *J. Nucl. Sci. Technol.* **2002**, *39* (6), 647−654.
(88) Spencer, S.; Gagliardi, L.; Handy, N. C.; Ioannou, A. G.; Skylaris, C.-K.; Willetts, A.; Simper, A. M. *J. Phys. Chem. A* **1999**, *103*, 1831−1837.
(89) Banisaukas, J.; Szczepanski, J.; Eyler, J. R.; Vala, M.; Hirata, S.; Head-Gordon, M.; Oomens, J.; Meijer, G.; von Helden, G. *J. Phys. Chem. A* **2003**, *107*, 782−793.
(90) Fielicke, A.; Mitric, R.; Meijer, G.; Bonacic-Koutecky, V.; von Helden, G. *J. Am. Chem. Soc.* **2003**, *125*, 15716−15717.
(91) Foresman, J. B.; Frisch, A. E. *Exploring Chemistry with Electronic Structure Methods*, 2nd ed.; Gaussian: Pittsburgh, PA, 1996.
(92) Langhoff, S. R. *J. Phys. Chem.* **1996**, *100*, 2819−2841.
(93) Aprà, E.; et al. *NWChem, A Computational Chemistry Package for Parallel Computers*, version 4.7; Pacific Northwest National Laboratory: Richland, WA, 2005.
(94) Kendall, R. A.; et al. *Comput. Phys. Commun.* **2000**, *128*, 260−283.
(95) Slater, J. C. *Phys. Rev.* **1951**, *81* (3), 385−390.
(96) Vosko, S. H.; Wilk, L.; Nusair, M. *Can. J. Phys.* **1980**, *58* (8), 1200−1211.
(97) Fuentealba, P.; Preuss, H.; Stoll, H.; Vonszentpaly, L. *Chem. Phys. Lett.* **1982**, *89* (5), 418−422.
(98) Fuentealba, P.; Vonszentpaly, L.; Preuss, H.; Stoll, H. *J. Phys. B: At. Mol. Opt. Phys.* **1985**, *18* (7), 1287−1296.
(99) Igel-Mann, G.; Stoll, H.; Preuss, H. *Mol. Phys.* **1988**, *65* (6), 1321−1328.
(100) Kaupp, M.; Schleyer, P. V.; Stoll, H.; Preuss, H. *J. Chem. Phys.* **1991**, *94* (2), 1360−1366.
(101) Dolg, M.; Stoll, H.; Preuss, H.; Pitzer, R. M. *J. Phys. Chem.* **1993**, *97* (22), 5852−5859.
(102) Küchle, W.; Dolg, M.; Stoll, H.; Preuss, H. *J. Chem. Phys.* **1994**, *100* (10), 7535−7542.
(103) Godbout, N.; Salahub, D. R.; Andzelm, J.; Wimmer, E. *Can. J. Chem.* **1992**, *70* (2), 560−571.
(104) Infante, I.; Visscher, L. *J. Comput. Chem.* **2004**, *25*, 386−392.
(105) Ziegler, T.; Rauk, A. *Inorg. Chem.* **1979**, *18* (7), 1755−1759.
(106) Ziegler, T.; Rauk, A. *Inorg. Chem.* **1979**, *18* (6), 1558−1565.
(107) Bickelhaupt, F. M.; Baerends, E. J. *Reviews in Computational Chemistry*; Wiley: New York, 2000; Vol. 15, pp 1−86.
(108) te Velde, G.; Bickelhaupt, F. M.; van Gisbergen, S. J. A.; Fonseca Guerra, C.; Baerends, E. J.; Snijders, J. G.; Ziegler, T. *J. Comput. Chem.* **2001**, *22*, 931−967.

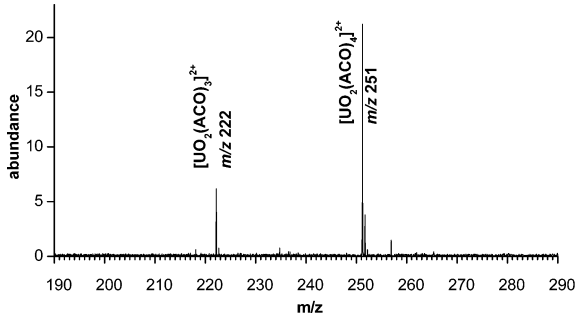

Figure 1. ESI mass spectrum of uranyl nitrate, 1 mM in a 50% acetone/water solution, spray temperature of 80 °C.

When the desolvation temperature was operated at modestly higher values (e.g., 100 °C), ions resulting from charge reduction reactions were observed to the exclusion of the uranyl dication complexes. Prior research using a quadrupole ion trap suggested that it should be possible to form the pentaligated uranyl−acetone complexes,[68] and in fact, these were observed when the desolvation temperature was decreased to near ambient (i.e., the block heater was turned off). However, ion instability prevented acquisition of IRMPD spectra for $n = 5$ acetone. We speculate that ion transmission from the electrospray needle to the ion accumulation region hexapole in the FT-ICR-MS deposits more energy into the ions than in the ion trap, thereby activating fast reverse reactions that have been observed in these species.[64]

The diligated acetone complex $[UO_2(ACO)_2]^{2+}$ was not observed directly from electrospray; however, it could be produced in sufficient abundance for IRMPD by mass isolating $[UO_2(ACO)_3]^{2+}$ using SWIFT[81] and then causing collision-induced dissociation using SORI.[79] Subsequent attempts to produce $[UO_2(ACO)_1]^{2+}$ using a similar strategy were not successful; instead, charge reduction occurred producing $[UO_2(ACO-H)]^+$. Thus, the envelope of $[UO_2(ACO)_n]^{2+}$ complexes available for IRMPD were $n = 2$, 3, and 4.

IR absorption bands were observed by photofragmentation of a SWIFT-isolated complex. In nearly all cases, fragmentation resulted in loss of an intact solvent ligand, as shown in eq 1 for the $n = 4$ acetone complex. The $n = 3$ complex behaved

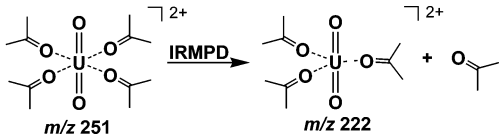

(1)

analogously. In contrast, the $n = 2$ complex decomposed by charge reduction, forming singly charged $[UO_2(ACO)]^+$ via a reaction that likely involved reduction of the uranium metal center and elimination of a charged (radical cation) acetone ligand (Figure 2, eq 2).

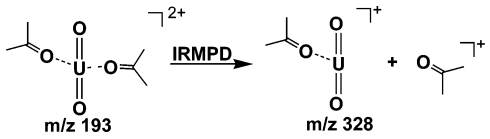

(2)

The high abundance of the $[UO_2(ACO)_4]^{2+}$ complex at *m*/*z* 251 produced a high signal-to-noise ratio in the IRMPD analysis, which enabled data acquisition across the entire mid-IR spectrum (Figure 3, solid red trace). The sharp O═U═O asymmetric

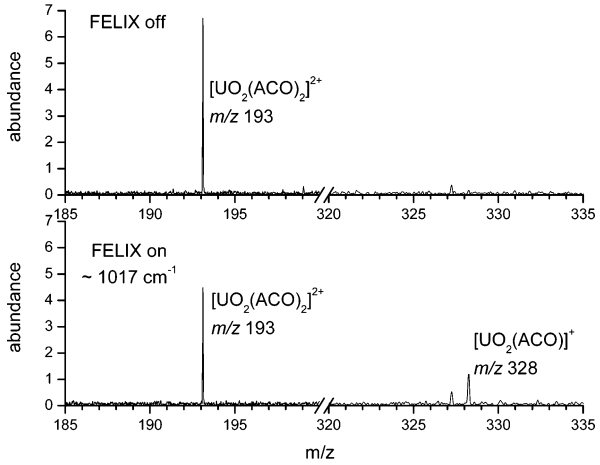

Figure 2. $[UO_2(ACO)_2]^{2+}$ formed by SORI CID of the $n = 3$ complex (upper spectrum) followed by FELIX irradiation and IRMPD (lower spectrum).

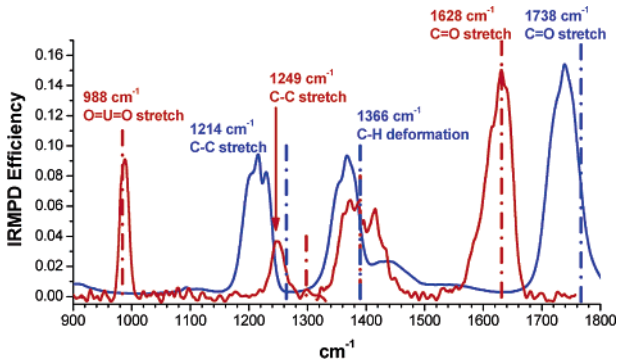

Figure 3. IRMPD spectrum of $[UO_2(ACO)_4]^{2+}$ (red), plotted with the NIST spectrum of gaseous acetone (blue). LDA theory was used to calculate IR frequency values for the complex and uncomplexed acetone which are indicated by the red-dashed and blue-dashed lines, respectively.

stretch at 988 cm^{-1} is the most outstanding feature at lower frequencies and is accompanied by frequencies derived from the acetone ligands. The frequencies of the latter peaks are shifted compared with those of unligated, gas-phase acetone[109] in a manner consistent with interaction of the carbonyl with the metal center. The carbonyl stretch observed at 1738 cm^{-1} in the spectrum of gas-phase acetone is red shifted to 1628 cm^{-1} in the uranyl−acetone complex, consistent with transfer of electron density to uranium and a weakening of the C═O bond. The weakened carbonyl, in turn, would be expected to shorten and strengthen the adjoining C−C bonds, which is consistent with the blue shift of the C−C stretch from 1214 cm^{-1} in acetone to 1249 cm^{-1} in the complex. Absorptions at the frequencies 1366 and 1438 cm^{-1} in the acetone spectrum are assigned to C−H deformations of the methyl groups.

The abundances of the $n = 3$ and $n = 2$ acetone complexes in the mass spectrum were lower than that of the $n = 4$, which caused a concomitant decrease in the signal-to-noise ratio in their IRMPD. Thus, lower precursor ion intensities for the $n = 2$ and $n = 3$ species necessitated collection of multiple FELIX shots for each data point. This in turn resulted in longer acquisition times, which made it necessary to focus data collection on the O═U═O and C═O stretching regions for these complexes.

(109) NIST Chemistry WebBook. http://webbook.nist.gov/cgi/cbook.cgi?ID=C67641& Units=SI&Mask=80#IR-Spec (accessed Feb 9).

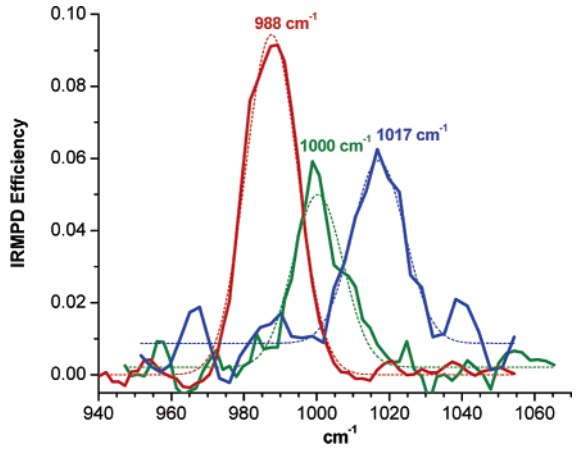

Figure 4. O═U═O stretching region of the IRMPD spectra of $[UO_2(ACO)_n]^{2+}$ Dotted lines are Gaussian fits, solid lines are data, for complexes having $n = 4$ (red), 3 (green), and 2 (blue).

Table 1. Uranyl, U−Acetone, U−Acetonitrile, and Acetone C═O Bond Lengths (in angstrom) for the Uranyl Acetone (ACO), Acetonitrile (ACN), and Mixed ACO/ACN Complexes Obtained from the Optimized LDA Structures

complex	U═O	U–ACO	C═O (ACO)	U–ACN
$[UO_2]^{2+}$	1.728			
Acetone			1.218	
$[UO_2(ACO)]^{2+}$	1.728	2.121	1.290	
$[UO_2(ACO)_2]^{2+}$	1.745	2.184	1.271	
$[UO_2(ACO)_3]^{2+}$	1.757	2.241	1.259	
$[UO_2(ACO)_4]^{2+}$	1.766	2.299	1.252	
$[UO_2(ACN)]^{2+}$	1.722			2.258
$[UO_2(ACN)_2]^{2+}$	1.735			2.310
$[UO_2(ACN)_3]^{2+}$	1.745			2.366
$[UO_2(ACN)_4]^{2+}$	1.754			2.415
$[UO_2(ACN)_5]^{2+}$	1.759			2.457
$[UO_2(ACN)_3(ACO)]^{2+}$	1.758	2.267/2.278	1.251	2.448
$[UO_2(ACN)_2(ACO)_2]^{2+}$	1.761	2.254	1.253	2.442
$[UO_2(ACN)(ACO)_3]^{2+}$	1.764	2.244	1.255	2.429/2.425
$[UO_2(ACN)_2(ACO)]^{2+}$	1.749	2.216	1.263	2.381
$[UO_2(ACN)(ACO)_2]^{2+}$	1.753	2.229	1.261	2.393

The O═U═O stretches were shifted to lower frequencies as the number of acetone ligands (n) in the $[UO_2(ACO)_n]^{2+}$ complexes increased from 2 to 3 to 4 (Figure 4). This shift is consistent with donation of additional electron density to the uranium center by each additional acetone, repelling the axial O atoms and thus weakening the U═O bonds. This interpretation is supported by the results of the computational modeling (Table 1) which shows a lengthening of the U═O bond, and a shortening of the acetone C═O bond, as more acetone or acetonitrile ligands are added. The magnitude of the red shift was greater for addition of the third acetone (17 cm^{-1}) than for the fourth acetone (12 cm^{-1}), indicating that the electron density per ligand donated to the metal center is greater in complexes containing fewer ligands. This conclusion concurs with the general observation that ligand binding energies in noncovalent metal−ligand complexes decrease as the number of ligands increases[110] and with molecular dynamics and DFT studies that showed greater uranyl−water distances for $[UO_2(H_2O)_5]^{2+}$ than for $[UO_2(H_2O)_4]^{2+}$.[44,111] Comparison of the magnitude of the red shifts caused by the acetone ligands with values measured in solution provides an indication of interactions of the solvent environment with the metal beyond those of the inner coordination sphere. The acetone-induced red shifts measured here for the asymmetric O═U═O stretch in gas-phase uranyl−acetone complexes were of the same magnitude (roughly 10−20 cm^{-1}) as the shifts correlated by Nguyen-Trung et al. for the Raman-active symmetric stretch upon addition of a donor ligand.[23]

The stretching frequency measured for the gaseous $[UO_2(ACO)_4]^{2+}$ complex (988 cm^{-1}) was about 23 cm^{-1} higher than the value for the aquo complex $[UO_2(H_2O)_5]^{2+}$ in solution, which was measured at 965 cm^{-1} in a low-pH perchlorate solution by Jones and Penneman in 1953.[16] It is in some sense surprising that this solution-phase measurement is so much lower than the value measured here for gas-phase $[UO_2(ACO)_4]^{2+}$, since acetone is a stronger nucleophile than H_2O[23,40,110] and therefore should more effectively donate electron density to the uranium center to cause a greater red shift. The difference might be attributed to the fact that the solution-phase pentaaquo complex has more electron donors (five)[112−115] complexed to the equatorial coordination sites than does the gas-phase four-acetone complex. However, the red shift in the uranyl frequency observed upon addition of the fourth acetone was only 13 cm^{-1}; the modest magnitude of the shift may reflect steric crowding of the equatorial ligands, which is suggested by a slight tilting of the acetone methyl groups out of the equatorial plane in the calculated B3LYP structures (Supporting Information, Figure S3). In the calculated LDA structure the acetone methyl groups stay in the equatorial plane, which can be attributed to LDA overestimating the hydrogen bonding strength (Figure S4 in the Supporting Information). A further red shift upon addition of a fifth acetone would be expected to be no more than an additional 13 cm^{-1}, and perhaps less; therefore, we would estimate that the frequency for the five-acetone complex would be not less than 975 cm^{-1}, which is still greater than the frequency of the ion in solution containing the more weakly binding water.

The lower frequency in solution must in part be due to the solvochromic effect, in which vibrational frequencies are red shifted in the presence of a dielectric solvent. To estimate the extent of this shift we carried out a self-consistent reaction field calculation for the uranyl dication in water using the Onsager model,[116−120] which predicted a red shift for the asymmetric stretch of ∼20 cm^{-1} using the dielectric constant for pure water. Because the dielectric constant in an ionic solution is lower,[121] the magnitude of the calculated solvochromic shift would be smaller, and hence 20 cm^{-1} represents the maximum adjustment. This would put the solvochromic-corrected value for the five-water complex at ∼985 cm^{-1}, which is only 10 cm^{-1} higher

(110) Rodgers, M. T.; Armentrout, P. B. *Mass Spectrom. Rev.* **2000**, *19* (4), 215−247.
(111) Shamov, G. A.; Schreckenbach, G. *J. Phys. Chem. A* **2005**, *109*, 10961−10974.
(112) Neuefeind, J.; Soderholm, L.; Skanthakumar, S. *J. Phys. Chem. A* **2004**, *108*, 2733−2739.
(113) Allen, P. G.; Bucher, J. J.; Shuh, D. K.; Edelstein, N. M.; Reich, T. *Inorg. Chem.* **1997**, *36*, 4676−4683.
(114) Semon, L.; Boeheme, C.; Billard, I.; Hennig, C.; Lutzenkirchen, K.; Reich, T.; Rossberg, A.; Rossini, I.; Wipff, G. *ChemPhysChem* **2001**, *2*, 591.
(115) Vallet, V.; Wahlgren, U.; Schimmelpfennig, B.; Moll, H.; Szabo, Z.; Grenthe, I. *Inorg. Chem.* **2001**, *40*, 3516−3525.
(116) Onsager, L. *J. Am. Chem. Soc.* **1936**, *58*, 1486−1493.
(117) Wong, M. W.; Frisch, M. J.; Wiberg, K. B. *J. Am. Chem. Soc.* **1991**, *113* (13), 4776−4782.
(118) Wong, M. W.; Wiberg, K. B.; Frisch, M. J. *J. Am. Chem. Soc.* **1992**, *114* (2), 523−529.
(119) Wong, M. W.; Wiberg, K. B.; Frisch, M. J. *J. Am. Chem. Soc.* **1992**, *114* (5), 1645−1652.
(120) Yu, G. S.; Freedman, T. B.; Nafie, L. A.; Deng, Z. Y.; Polavarapu, P. L. *J. Phys. Chem.* **1995**, *99* (2), 835−843.
(121) Hasted, J. B.; Ritson, D. M.; Collie, C. H. *J. Chem. Phys.* **1948**, *16* (1), 1−21.

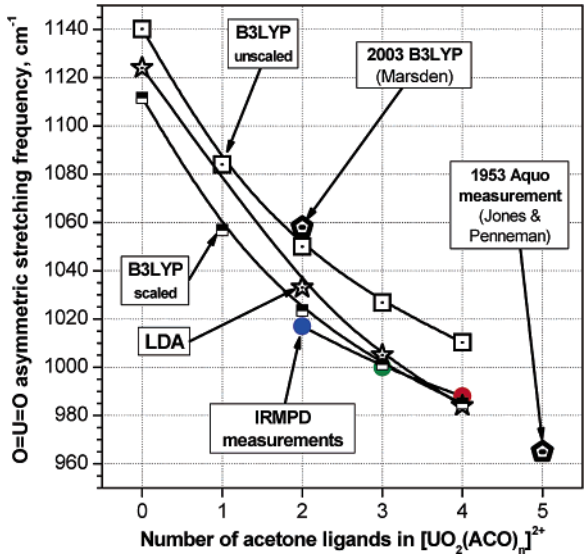

Figure 5. Comparison of IRMPD asymmetric O═U═O stretching frequencies for the $[UO_2(ACO)_{n=2,3,4}]^{2+}$ complexes (circles) with the unscaled results of LDA calculations (stars), B3LYP unscaled calculations (squares), and B3YLP scaled calculations (half-filled squares). The results of Marsden's 2003 B3LYP calculation for $n = 2$ and the original measurement for the solution-phase aquo complex are included for comparison.

than the lowest value estimated for the five-acetone complex. The results suggest, therefore, that the uranyl stretch of the water complexes are further influenced by additional solution interactions that could be either in the equatorial plane or perhaps with the axial oxygen atoms in a manner analogous to the Lewis acid binding recently reported.[122,123] A combined quantum chemical−molecular simulation study[44] also suggested that the second solvation shell may donate a modest amount of additional electron density at the uranium center.

A direct comparison of the aqueous uranyl frequency with that of a gas-phase water complex would be desirable to facilitate a more valid comparison. However, attempts to stabilize aquo complexes in the FT-ICR-MS were unsuccessful, in accord with the computational results indicating that the $[UO_2(H_2O)_2]^{2+}$ complex has a lower coordination energy than its acetone counterpart.[40] In past attempts to generate gas-phase, uranyl−aquo complexes (i.e., $[UO_2(H_2O)_n]^{2+}$) by ESI, the mass spectra have been dominated by hydrated uranyl−anion complexes such as $[UO_2OH(H_2O)_n]^+$ and $[UO_2NO_3(H_2O)_n]^+$, even when weakly coordinating anions such as ClO_4^- were used.[62,63,66,67] These experimental difficulties have limited direct comparisons of O═U═O stretching frequencies for complexes in solution with those in the gas phase; however the lower frequency expected for the acetone complexes (compared to similarly ligated water complexes) was supported by direct comparison of computationally generated frequencies for the four-water and four-acetone complexes.

A plot of the O═U═O stretching frequency versus the number of ligands attached reveals a systematic red shifting that was effectively modeled using both LDA and B3LYP approaches, and a comparison is shown in Figure 5. The frequency measured in solution for $[UO_2]^{2+}$ (965 cm^{-1} in a low-pH perchlorate solution,[16] thought to be a pentaaquo complex[112−115]) is also shown to provide historical and spectroscopic context. The IRMPD measurements of the gas-phase uranyl complexes are not influenced by the dynamic interactions occurring in solution[43,44] and hence provide excellent calibration points for the theoretical methods. Experimental validation studies are needed because modeling actinide structures has historically been challenging on account of the large number of electrons involved, relativistic effects, and spin−orbit coupling.[10,41,124,125]

The LDA calculations have had success in modeling uranyl vibrational frequencies[37,38,42] and were performed for the $[UO_2(ACO)_{n=2,3,4}]^{2+}$ complexes. In the optimized LDA structures of the tri- and tetraacetone complexes the uranyl unit is linear, and the acetones are symmetrically distributed in the equatorial plane. All carbon and carbonyl oxygen atoms lie in the equatorial plane. The ligand−uranyl−ligand angle in the diacetone complex is bent with an angle of 117°, and the O═U═O is slightly distorted from linear (angle 177°) with the uranyl oxygen atoms bent away from the acetones. The unscaled values for the O═U═O and C═O stretching frequencies for the $n = 4$ complex were within a few cm^{-1} of the IRMPD values (Figures 3, 5; tabulations and assignments for frequencies calculated for all complexes are found in Tables S3−S16 in the Supporting Information). The LDA-calculated value for the O═U═O stretch (984 cm^{-1}) for the $n = 4$ acetone complex can be compared with a value of 1024 cm^{-1} calculated for the $n = 4$ water complex using the same theoretical method.[126] In fact, the asymmetric stretch frequencies for the $n = 2-5$ water complexes are found to be ∼40 cm^{-1} higher than the corresponding acetone complexes and ∼15 cm^{-1} higher than the corresponding acetonitrile complexes. These results support the expectation that acetone is a stronger gas-phase nucleophile than water, which in turn indicates that for complexes in aqueous solution, different structures (i.e., with ligands not oriented in the equatorial plane) or additional interactions are responsible for further lowering the O═U═O frequency measured in solution.

The LDA-calculated C−C stretching frequency for the $n = 4$ acetone complex was approximately 50 cm^{-1} higher than the IRMPD measurement, which was the same variation that was observed in a comparison of the IR spectrum of free acetone with the LDA-calculated value (Figure 3). LDA-calculated frequencies for the C−H deformations were in close agreement with the broadened peak that was recorded in the IRMPD experiments for the $n = 4$ complex. The calculated asymmetric uranyl stretching frequencies (unscaled) of the $n = 3$ and $n = 2$ complexes were 5 and 16 cm^{-1} higher (respectively) than the measurements (Figure 5, tabulated values in Supporting Information Table S1).

The frequencies were also modeled at the B3LYP level of theory. The SDD basis set was employed for uranium[63,87,88] and the 6-31+G(d) for all other elements (results also presented in Figure 5). With the use of this approach, the unscaled value for the $[UO_2(ACO)_2]^{2+}$ complex was in near-perfect agreement with previous B3LYP calculations[40] and 33 cm^{-1} higher than the IRMPD measurement. The difference between the unscaled calculations and measurements decreased to about 20 cm^{-1} as

(122) Albrecht-Schmitt, T. E.; Almond, P. M.; Sykora, R. E. *Inorg. Chem.* **2003**, *42*, 3788−3795.
(123) Sarsfield, M. J.; Helliwell, M. *J. Am. Chem. Soc.* **2004**, *126*, 1036−1037.
(124) Infante, I.; Visscher, L. *J. Chem. Phys.* **2004**, *121* (12), 5783−5788.
(125) de Jong, W. A.; Visscher, L.; Nieuwpoort, W. C. *J. Mol. Struct.* **1999**, *458*, 41−52.
(126) Zhang, Z.; de Jong, W. A.; Windus, T. L. 2006.

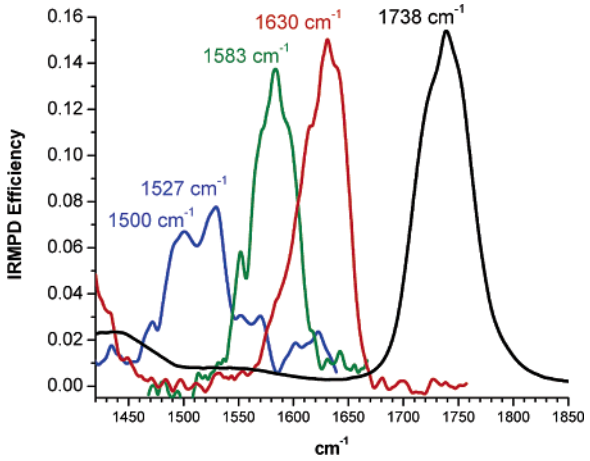

Figure 6. C═O stretching region of the IRMPD spectra of $[UO_2(ACO)_n]^{2+}$ where $n = 4$ (red), $n = 3$ (green), $n = 2$ (blue), and the IR spectrum of uncomplexed gas-phase acetone (black).

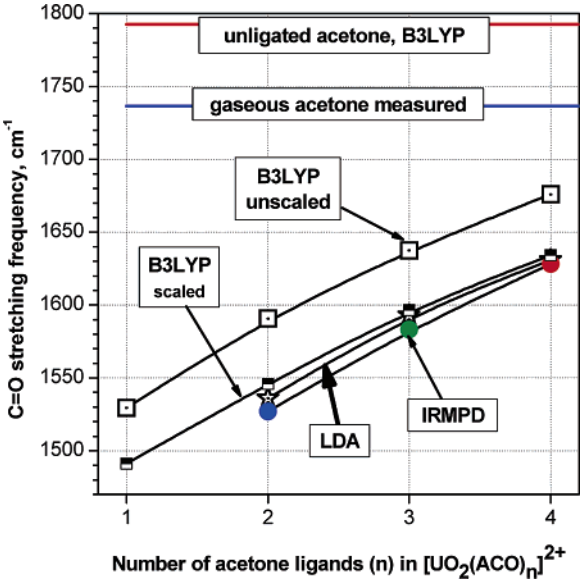

Figure 7. Comparison of the C═O stretching frequencies of the IRMPD spectra of $[UO_2(ACO)_n]^{2+}$ with uncorrected values calculated using LDA and B3LYP methods.

the number of acetone ligands increased from two to three and then four. As noted in the Experimental Section, modest scaling factors are commonly applied to the frequency values generated from B3LYP calculations. Scaling by a factor of 0.975 resulted in very close agreement of the B3LYP and IRMPD values (Figure 5).

The trend toward lower frequencies noted for the O═U═O stretch as n increased in the $[UO_2(ACO)_n]^{2+}$ complexes was mirrored by the behavior of the C═O stretch, which systematically moved to higher frequencies (Figure 6). As more acetone ligands are added to the metal center, each ligand contributes less electron density, causing the C═O stretching frequency for the $n = 4$ complex to more closely resemble that of the uncomplexed acetone. This trend can also be seen in Table 1, where the C═O bond length is shortened as more acetone ligands are added. For the $n = 2$ complex, the carbonyl groups of the acetone ligands are perturbed as a consequence of transfer of substantial electron density to the metal and have two maxima, the most intense of which is at 1527 cm^{-1} and the less intense at ~1500 cm^{-1}. The origin of this phenomenon may be the result of symmetric and asymmetric coupling of two individual C═O stretches, which is what was indicated by the LDA (Table S4 in the Supporting Information) and B3LYP calculations. The frequency of the asymmetric coupling was predicted to have a small intensity; however, coupling with different vibrational modes might enhance this. The splitting between the two is 24 cm^{-1}, which is close to what is observed experimentally. Addition of the third acetone weakens uranyl−ligand binding, which blue shifts the C═O stretching frequency to 1583 cm^{-1}, about 155 cm^{-1} lower than that of unligated acetone. The shape of the C═O absorption in the $n = 3$ acetone complex shows a narrow shoulder at ~1551 cm^{-1}. Although the shoulder was close to the noise level in this experiment, there were two data points in the IRMPD spectrum that were clearly more intense than neighboring points, and the overall profile of the C═O stretch suggested the presence of a second band reminiscent of what was seen for the $n = 2$ complex. However, the calculations did not predict a second band in the $n = 3$ (or $n = 4$) acetone complex(es). Finally, addition of the fourth acetone produces a clearly defined absorption at 1628 cm^{-1}, 110 cm^{-1} lower than that of unligated acetone. This peak does not show a second maxima but is broadened on the lower frequency side, suggesting the presence of an unresolved absorption band.

The shift to higher frequency with an increasing number of acetone ligands was reproduced using both the LDA and the B3LYP calculations (Figure 7, tabulated values in Table S2); we selected the more intense and higher frequency value measured for the $n = 2$ acetone complex (at 1527 cm^{-1}) for comparison with the calculations. The unscaled LDA-generated values were in close agreement with the IRMPD measurements. The unscaled B3LYP calculations produced a trend that was very close to that of the measurements and were more energetic by about 50 cm^{-1} for the same complexes; when the B3LYP scaled, values were within ~10 cm^{-1} of the measurements. Values calculated for the $n = 2$ complex using either method were less accurate; however, this conclusion is tempered as a result of the irregular or superimposed peak shape noted above.

IRMPD of Uranyl−Acetonitrile (ACN) Complexes. Complexation of a more modest nucleophile to the uranyl center should produce a smaller shift in the O═U═O frequency, and the IRMPD spectra of acetonitrile complexes enabled this expectation to be directly investigated. The previous B3LYP study[40] of diligated complexes predicted the diacetonitrile uranyl complex to be 19 cm^{-1} higher than the analogous diacetone complex. The mass spectrum produced by ESI of a uranyl/acetonitrile/H_2O solution contained an ion at m/z 217 corresponding to $[UO_2(ACN)_4]^{2+}$ and a less abundant $[UO_2(ACN)_5]^{2+}$ at m/z 237.5. The triligated $[UO_2(ACN)_3]^{+}$ was formed using a SWIFT/SORI sequence, albeit at a significantly lower intensity compared with the parent $n = 4$ complex ion. The diligated complex could not be generated in sufficient intensity, using a second SWIFT/SORI stage, and thus the envelope of uranyl−ACN species investigated by IRMPD included those with three, four, and five ligands.

Because of the low precursor ion intensities, and resulting long IR acquisition time, data collection was focused on the O═U═O asymmetric stretching frequency (ca. 1000 cm^{-1}) (Figure 8). Despite low signal-to-noise ratio (due to low ion intensity and low IRMPD efficiency), the uranyl stretching

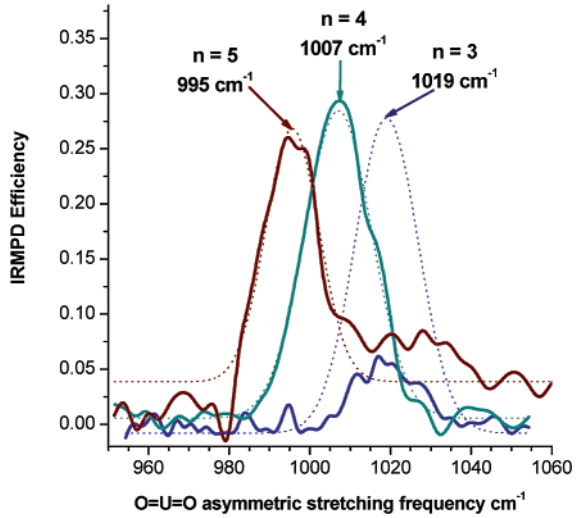

Figure 8. O═U═O stretching region of the IRMPD spectra of $[UO_2(ACN)_n]^{2+}$ for complexes having $n = 5$ (red), $n = 4$ (teal), and $n = 3$ (blue). Solid lines are data, dotted lines are Gaussian fits (fit for the $n = 3$ complex is scaled by 5× to facilitate comparison).

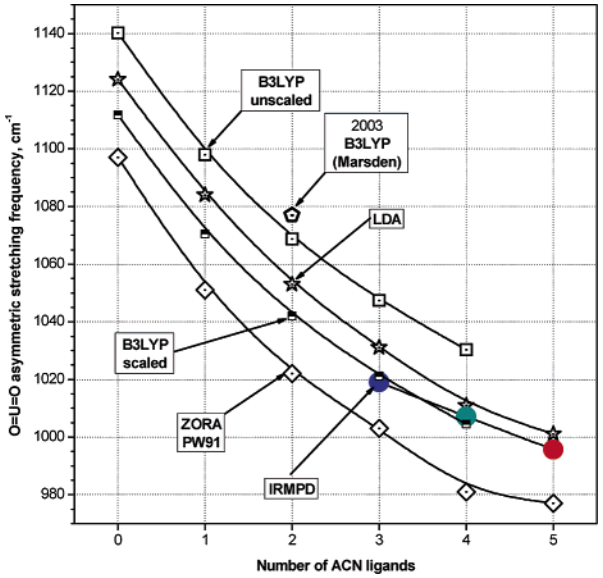

Figure 9. Comparison of O═U═O asymmetric stretching frequencies for the $[UO_2(ACN)_n]^{2+}$ complexes measured using IRMPD and calculated using B3LYP (scaled and unscaled), LDA, and ZORA-PW91 levels of theory.

frequency for the $n = 3$ complex could be readily measured at 1019 cm^{-1}, which was 19 cm^{-1} higher than that measured for the analogous $[UO_2(ACO)_3]^{2+}$ (Figure 4); this difference clearly indicates that acetonitrile is a weaker nucleophile and is in excellent agreement with the difference predicted between the diligated ACO and ACN complexes.[40] Increasing the number of ACN ligands to four and then five resulted in the uranyl stretch shifting to lower frequency by 12 cm^{-1} in each step. The fact that the magnitude of the red shifts were (a) equivalent to the magnitude of the shifts observed in a comparison of the tri-ACO and tetra-ACO complexes and (b) were not decreasing with increasing n (as they were in the all-ACO complexes) suggests that repulsive steric interactions may in fact be weakening binding of the ACO (note that the calculated structures for $[UO_2(ACO)_4]^{2+}$ show slight repulsion of methyl groups out of the equatorial plane, Figure S3). Steric repulsion is probably not important in the ACN complexes, and hence addition of a fourth ACN ligand to $[UO_2(ACN)_3]^{2+}$ effects a red shift in the O═U═O frequency whose magnitude is equivalent to that effected by addition of a fourth ACO ligand to $[UO_2(ACO)_3]^{2+}$. This result was surprising since ACN is a weaker nucleophile and points to the fact that ACN is less influenced by steric crowding at the metal center than is ACO.

As with the acetone complexes, the stretching frequencies generated for the ions in the $[UO_2(ACN)_{n=3-5}]^{2+}$ series provided a valuable benchmark for comparison with frequencies generated computationally (Figure 9, tabulated values in Table S1). For the uranyl−ACN complexes, calculations were conducted at the LDA, ZORA-PW91,[104] and B3LYP levels of theory. As was the case for the larger acetone complexes, in the LDA structures of the tri-, tetra-, and pentaacetonitrile complexes the uranyl unit is linear and the acetones are symmetrically distributed in the equatorial plane, with all carbon and nitrogen atoms in this plane. The ligand−uranyl−ligand angle in the diacetonitrile complex is bent with an angle of 104°, and the O═U═O bond angle is slightly deformed (angle 176°) with the uranyl oxygen atoms being slightly repelled away from the acetonitrile molecules. The unscaled LDA frequencies were in very good agreement with the IRMPD measurements for the $n = 4$ and $n = 5$ complexes (within 4−5 cm^{-1}) and were ∼12 cm^{-1} higher than the IRMPD frequency for the $n = 3$ complex. The unscaled uranyl stretching frequencies generated using B3LYP were about 20−30 cm^{-1} higher than the IRMPD measurements, which appears to be a general conclusion since the difference between theory and experiment here was similar to that observed in the all-ACO complexes. When scaled by 0.975, the B3LYP results were in excellent agreement. The unscaled ZORA-PW91 were 16−19 cm^{-1} lower than experimental values, which is consistent with the fact that this functional gives smaller frequencies for the bare uranyl as compared to those of reference coupled cluster calculations.[37,127]

The differences between the LDA, B3LYP, and ZORA-PW91 calculations are attributed primarily to the DFT functional chosen. To get an estimate of the basis set effects and effects from the ZORA approximation additional NWChem calculations were performed using the PW91 and B3LYP functionals with the same basis sets used for the LDA calculations. Vibrational frequencies for only the diacetone and diacetonitrile complexes were calculated for comparison. The uranyl asymmetric stretch for the acetonitrile complex obtained with NWChem using the B3LYP and PW91 functional are 1076 and 1029 cm^{-1}, respectively. These results are in close to the Gaussian B3LYP result of 1069 cm^{-1} and the ADF ZORA-PW91 result of 1022 cm^{-1}. The acetone asymmetric stretch of 1055 cm^{-1} from NWChem with the B3LYP functional is close to the Gaussian B3LYP number of 1050 cm^{-1}. Hence, the basis set errors introduced are much smaller than the differences seen when comparing the results of the B3LYP and PW91 with those of LDA, confirming that those differences are due to the functional chosen.

The curves plotted from the frequency shifts from all three methods agreed reasonably well, giving the same qualitative trend and ending at a different bare uranyl stretching frequency. Previous DFT studies emphasized bond energy decomposition analyses on an extensive range of diligated complexes, which

(127) de Jong, W. A.; Harrison, R. J.; Nichols, J. A.; Dixon, D. A. *Theor. Chem. Acc.* **2002**, *107*, 318.

Table 2. Uranyl−Acetonitrile Bond Energy Values Derived from Decomposition Analyses of the $[UO_2(ACN)_{n=1,2,4}]^{2+}$ Based on the ZORA-PW91 and Electrostatic Model Calculations

no. of ACN ligands	ZORA-PW91 kcal mol^{-1}	electrostatic kcal mol^{-1}
1	100.5	93.7
2	80.7	80.5
3	78.5	76.1
4	70.1	70.0
5	62.0	64.1

suggested that while polarization and charge transfer were important, the dominant factor was the electrostatic component.[40] While acetonitrile was not explicitly discussed, it had one of the highest dipole moments of all ligands in the study, and hence its binding would also be expected to have a large electrostatic component. With the use of the optimized geometries for the all-ACN complexes, a Ziegler−Rauk type energy decomposition[106,128] was performed (neglecting deformation energy of the acetonitrile ligand, which contributes only a few kcal mol^{-1} to the overall result (1.6 kcal mol^{-1} for acetonitrile in the monocoordinated structure)). The bond energy per ligand decreased from ∼100 kcal mol^{-1} for $[UO_2(ACN)]^{2+}$ to ∼64 kcal mol^{-1} for $[UO_2(ACN)_5]^{2+}$. The bond energy calculated here for the diligated complex (80.7 kcal mol^{-1}) was within a few kcal mol^{-1} of the complexation energy calculated in the earlier B3LYP study.[40] The bond energy decomposition suggested that these complexes can be modeled using primarily electrostatic terms (Table 2), since the large Pauli repulsion and orbital interaction terms almost completely cancel each other. This reflects the fact that the electron density does not change much upon going from the promolecule, in which the densities of the uranyl and ACN ligands are simply superimposed, to the real molecule. Orbital decomposition does, however, show the participation of the empty 5f and 6d orbitals of uranium in the final orbitals, needed to achieve orthogonality on the closed-shell uranyl core. This is conventionally interpreted as ligand-to-metal charge transfer. The large uranyl frequency shifts are due to this charge transfer that lengthens and weakens the uranium−oxygen bonds.

IRMPD of Uranyl−Mixed Acetonitrile−Acetone Complexes. Uranyl−mixed solvent complexes were also generated in these experiments, originally from traces of residual acetone in the spray chamber, but later deliberately formed by addition of acetone vapor. The generalized formula for the mixed complexes was $[UO_2(ACN)_m(ACO)_n]^{2+}$, where $m + n = 4$. Mixed solvent complexes were observed despite the fact that ACN was in vast excess (in the spray solvent), because ACO is a much stronger nucleophile compared with ACN and displaced the ACN in the originally formed complexes during the long time period (∼0.5 s) ions spend in the hexapole ion accumulation chamber. The formation of the mixed complexes afforded the opportunity to examine the influences of small changes in the ligand field on the uranyl stretching frequency. Multiple SWIFT isolation windows were simultaneously imposed that enabled collection of IRMPD spectra of four separate complexes at the same time. The $[UO_2(ACN)_4]^{2+}$ at *m*/*z* 217.1, $[UO_2(ACN)_3(ACO)_1]^{2+}$ at *m*/*z* 225.6, $[UO_2(ACN)_2(ACO)_2]^{2+}$ at *m*/*z* 234.1, and $[UO_2(ACN)_1(ACO)_3]^{2+}$ at *m*/*z* 242.6 were isolated and subjected to photodissociation. This caused elimination of acetonitrile (the more weakly bound ligand) in each case (Figure 10). With one exception, photofragments that were generated were not isobaric with each other or with the undissociated complexes. The exception arose from the presence of a low-abundance ion at *m*/*z* 251.1, which corresponded to $[UO_2(ACO)_4]^{2+}$, for which the photodissociation product ion $[UO_2(ACO)_3]^{2+}$ was identical to that of $[UO_2(ACN)_1(ACO)_3]^{2+}$. However, the IRMPD spectrum of the $[UO_2(ACN)_1(ACO)_3]^{2+}$ complex was not significantly compromised because the abundance of the $[UO_2(ACO)_4]^{2+}$ was low in this experiment, and furthermore the all-ACO ions have showed lower IRMPD efficiencies (vide infra).

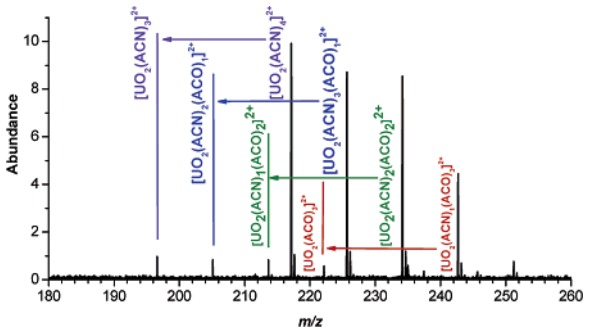

Figure 10. Mass spectra of mixed acetonitrile/acetone uranyl complexes $[UO_2(ACN)_m(ACO)_n]^{2+}$ (where $m + n = 4$) isolated using SWIFT and photofragmented at 995 cm^{-1}. The experiment simultaneously produced IRMPD spectra for four different complexes.

Examination of the uranyl stretch for the mixed complexes $[UO_2(ACN)_m(ACO)_n]^{2+}$ ($m + n = 4$) reinforced the earlier conclusion that substitution of a more nucleophilic ligand resulted in a red shift in the O═U═O frequency (Figure S1 in the Supporting Information). The all-ACN complex ($m = 4$, $n = 0$) was measured at 1007 cm^{-1} (Figure 8); substitution of one ACN for one ACO produced the ($m = 3$, $n = 1$) complex which resulted in a red shift of ∼6 to 1001 cm^{-1}, consistent with the stronger nucleophilic character of ACO. Sequential substitution of the second, third, and finally fourth ACN ligands with ACO produced asymmetric frequencies of 995, 991, and 988 cm^{-1} corresponding to consecutive red shifts of decreasing magnitude, 6, 4, and 3 cm^{-1} for the ($m = 2$, $n = 2$), ($m = 1$, $n = 3$), and ($m = 0$, $n = 4$) complexes, respectively. The results underscore the sensitivity of the O═U═O stretching frequency for recording relatively subtle changes in the ligand field of the complex.

The IRMPD efficiency appears to be decreasing as more acetone is incorporated. This was suggested by comparison of efficiencies at the uranyl stretching frequencies of all-ACN complexes with those of the all-ACO complexes: for example the efficiency of the $[UO_2(ACN)_4]^{2+}$ photofragmentation (Figure 8) is about 3 times greater than that of $[UO_2(ACO)_4]^{2+}$ (Figure 4). The trend was reinforced in the uranyl−mixed ligand experiment (Figure S1), where the efficiency generally decreases as additional ACO ligands are substituted for ACN ligands. Here the comparison is better because the complexes were subjected to identical photofragmentation conditions. The result indicates that poorer photofragmentation efficiency is correlated with higher ligand binding energies.

Comparison of the O═U═O stretching frequencies measured for the ($m + n = 4$) mixed ligand complexes with unscaled LDA-calculated values produced remarkable agreement: all

(128) Ziegler, T.; Rauk, A. *Theor. Chim. Acta* **1977**, *46* (1), 1−10.

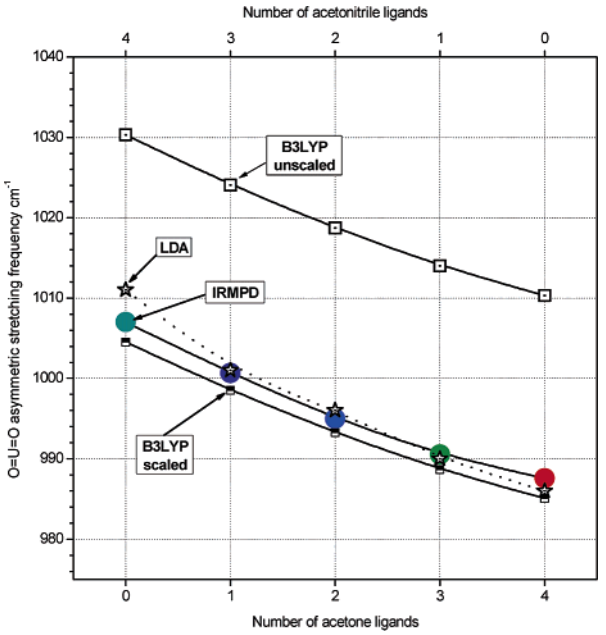

Figure 11. Comparison of O═U═O asymmetric stretching frequencies for the $[UO_2(ACN)_m(ACO)_n]^{2+}$ complexes ($m + n = 4$) measured using IRMPD and calculated using B3LYP and LDA levels of theory.

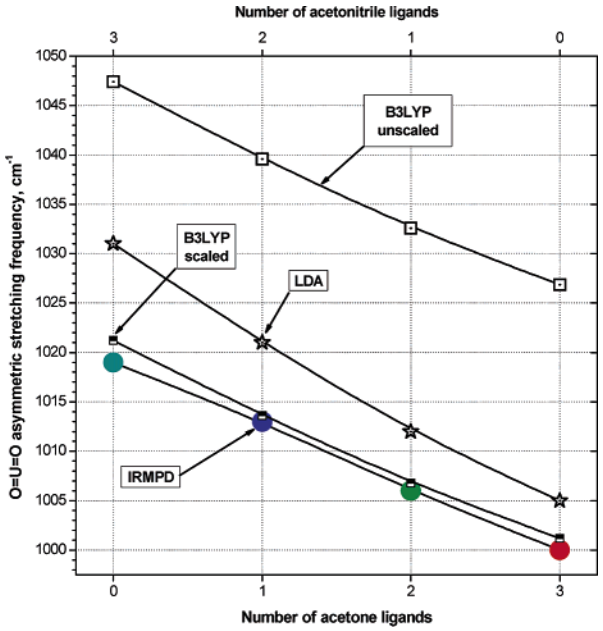

Figure 12. Comparison of O═U═O asymmetric stretching frequencies for the $[UO_2(ACN)_m(ACO)_n]^{2+}$ complexes ($m + n = 3$) measured using IRMPD and calculated using B3LYP and LDA levels of theory.

LDA-calculated values were within 4 cm^{-1} of experimental measurements (Figure 11, tabulated values in Table S1). This points to the accuracy achievable for the metal−oxygen frequency using this approach. The agreement between the unscaled B3LYP-calculated frequencies and the measurements was also very good; in this comparison, the calculations were ~23 cm^{-1} more energetic for all five tetraligated complexes compared, which showed that the trending was well modeled using this approach. When scaled, the B3LYP frequencies were actually about 5 cm^{-1} lower than the measurements.

The triligated, mixed solvent uranyl complexes formed as products of IRMPD of the tetraligated species (see Figure 10) could also be formed using collision-induced dissociation using a SWIFT/SORI sequence. Although substantial ion abundance was lost in the isolation/fragmentation process, a series of ions having the general formula $[UO_2(ACN)_m(ACO)_n]^{2+}$ where $(m + n) = 3$ were formed in sufficient abundance for IRMPD experiments. Because of lower ion abundance and IRMPD efficiency for the triligated complexes, their IRMPD spectra had lower signal-to-noise ratios than the tetraligated species. When the complexes containing ACN were irradiated at the O═U═O frequency, they fragmented by loss of ACN (as did the tetraligated mixed ACN/ACO complexes). The O═U═O stretching frequencies (Figure S2 in the Supporting Information) displayed trends that were similar to those of the tetraligated complexes, in that the uranyl stretch was progressively red shifted as (a) the number of acetone ligands increased and (b) the number of acetonitrile ligands decreased. The magnitude of the red shift observed on substitution of an ACO for and ACN in the $(m + n) = 3$ complexes was 6−7 cm^{-1} in each instance. The photofragmentation efficiency was substantially less than in the case of the $(m + n) = 4$ complexes, which probably also reflects stronger uranium−ligand binding for the $(m + n) = 3$ complexes.

The O═U═O stretching frequencies for the $(m + n) = 3$ complexes were calculated using LDA and B3LYP methods and compared with the IRMPD values (Figure 12, tabulated values in Table S1) The unscaled frequencies calculated using LDA were slightly greater than the measurements, with the differences ranging from 12 cm^{-1} for the all-ACN complex to 5 cm^{-1} for the all-ACO complex. For both the tetraligated and triligated complexes the O═U═O angle is very close to linear, with the carbons, oxygen (acetone), and nitrogen (acetonitrile) atoms of the ligands in the equatorial plane. The unscaled B3LYP frequencies were consistently 26−27 cm^{-1} greater than the measurements, reproducing the trend upon ACN-for-ACO substitution. Excellent accuracy was achieved when the frequency values were scaled.

Conclusions

The results of this study are the first vibrational spectra measured for gas-phase uranyl ion complexes. A strong absorption attributed to the asymmetric O═U═O stretch was observed for a range of uranyl−acetone, uranyl−acetonitrile, and uranyl−mixed ligand complexes. The uranyl asymmetric stretching frequencies systematically shifted to lower values as the number of equatorial ligands within the precursor complex increased, and with increasing ligand nucleophilicity. For acetone complexes, as the number of ligands increases, the red shift observed in the uranyl frequency was complemented by blue shift for the carbonyl stretch, signaling decreasing transfer of electron density from coordinating ligand to the uranium center with increasing extent of ligation. These measurements provide explicit benchmark values that were compared with results of three different theoretical calculations, which have been historically difficult for actinide species on account of the large number of electrons involved, relativistic effects, and spin−orbit coupling.

For the unscaled calculated frequencies, the best agreement was achieved using the LDA approach, which provided unscaled uranyl frequency values that were within a few cm^{-1} of the IRMPD values. B3LYP using a combination of SDD and

6-31+G(d) basis sets also generated unscaled uranyl frequencies that were in very good agreement with the measurements, being 20−30 cm^{-1} higher. The trends observed in the data in general appeared to be best reproduced by the B3LYP method and, when appropriately scaled, provided excellent accuracy. The unscaled uranyl frequencies calculated for the all-acetonitrile complexes using ZORA-PW91 were also in very good agreement, being about 20 cm^{-1} lower, and accurately reproducing trending in the measured frequencies. The theoretical results are highly encouraging since it is hoped that these computational approaches will effectively account for relativistic effects and spin−orbit coupling that are encountered in calculation of more complex systems.

Acknowledgment. Work by G. S. Groenewold and A. K. Gianotto was supported by the U.S. Department of Energy, Assistant Secretary for Environmental Management, and the INL Laboratory Directed Research and Development Program under DOE Idaho Operations Office Contract DE-AC07-05ID14517. The INL authors thank the University of Florida (Professor John Eyler) for travel support. M. J. Van Stipdonk was supported through a Grant from the U. S. National Science Foundation (NSF Grant CAREER-0239800). The FOM authors were supported by the Nederlandse Organisatie voor Wetenschappelijk Onderzoek. The skillful assistance by the FELIX staff, in particular Dr. B. Redlich, is gratefully acknowledged. Construction and shipping of the FT-MS instrument was made possible through funding from the National High Field FT-ICR Facility (Grant CHE-9909502) at the National High Magnetic Field Laboratory, Tallahassee, FL. W. A. de Jong's research was performed in part using the Molecular Science Computing Facility in the William R. Wiley Environmental Molecular Sciences Laboratory, a national scientific user facility sponsored by the U.S. Department of Energy's Office of Biological and Environmental Research located at the Pacific Northwest National Laboratory, which is operated for the Department of Energy by Battelle. L. Visscher thanks the Netherlands Organization for Scientific Research (NWO) for financial support through the "Jonge Chemici" program.

Supporting Information Available: Three additional figures providing details on the results from IRMPD experiments and calculated structures of two complexes; the atomic coordinates for the optimized LDA geometries, the complete set of vibrational frequencies (and their assignments) in the experimental range, and the calculated frequencies for the LDA, B3LYP, and PW91 results used in the figures; complete citations for refs 82, 93, and 94 are shown. The material is available free of charge via the Internet at http://pubs.acs.org.

JA058106N